Quantum chemical calculations of lupeol ($C_{30}H_{50}O$) isolated from the ethyl acetate leaf extracts of *Justicia Secunda*

B. Bako[a,b], E. E. Etim[a,b,*], J. P. Shinggu[a,b], S. S. Humphrey[a,b], L. J. Moses[a,b], M. E. Khan[c]

[a]*Computational, Astrochemistry and Bio-simulation Research Group, Federal University Wukari, Wukari, Nigeria*
[b]*Department of Chemical Sciences, Federal University Wukari, Wukari, Nigeria*
[c]*Department of Chemistry, Federal University Lokoja, Kogi, Nigeria*

Abstract

The discovery of lupeol, a triterpenoid compound ($C_{30}H_{50}O$), in the ethyl acetate leaf extract of *Justicia secunda* (Blood root), has opened doors to extensive research and development opportunities in natural product-based pharmaceuticals. Lupeol's versatile pharmacological properties, including anti-inflammatory, anticancer, antidiabetic, and antiviral effects, make it a compelling candidate for drug development. To fully harness its potential, a comprehensive understanding of lupeol's structural and chemical attributes is crucial. Through quantum chemical calculations using the GAUSSIAN 09 suite of programs, we determined the optimized geometry, IR frequencies, bond distances (R), bond angles (A), dipole moments, HOMO-LUMO and other molecular parameters for this solitary molecule. The remarkable accuracy and reliability of computational techniques in predicting the properties of systems and reactants are evident in the consistently favorable results. A strong concordance and consistency between the experimental and computational outcomes further reinforces the credibility of our findings. This study offers a means to explore lupeol's molecular behavior, providing insights that can guide future drug development efforts rooted in this promising natural compound.

Communicated by: B. J. Falaye

1. Introduction

Natural products have always served as a wellspring of inspiration for the field of drug discovery and development [1–4]. Among these, *Justicia secunda*, commonly referred to as Blood root, has gained prominence for its historic use in traditional medicine across different cultures [5, 6]. *Justicia secunda* has been esteemed for its therapeutic potential, encompassing anti-inflammatory, antioxidant, and anticancer proper-

ties [7–10]. One of the primary compounds identified in the ethyl acetate leaf extract of *Justicia secunda* is lupeol, a triterpenoid with the chemical formula $C_{30}H_{50}O$ a melting point of 215-216 °C [11].

Lupeol, as a natural compound, has recently attracted considerable attention owing to its versatile pharmacological attributes and potential applications within the pharmaceutical sector [12, 13]. This compound has been documented to display a broad spectrum of biological functions, including anti-inflammatory, anticancer, antidiabetic, and antiviral effects [14–16]. The uncomplicated molecular structure of lupeol, coupled

*Corresponding author Tel. No.: +234-907-919-2231.
Email address: etim@journal.nsps.org.ng (E. E. Etim)

with its promising pharmacological characteristics, renders it an enticing candidate for further investigation and integration into drug development endeavors.

Computational chemistry is a pivotal discipline that bridges the realms of theoretical chemistry and practical applications in various scientific fields, including pharmaceutical research. It plays an indispensable role in understanding and predicting the behavior of molecules and chemical processes at the atomic and molecular levels, offering valuable insights that are often challenging to obtain through traditional experimental methods alone [17, 18]. The identification of lupeol within the ethyl acetate leaf extract of *Justicia secunda* presents promising avenues for exploration and advancement in the realm of pharmaceuticals derived from natural products. Nevertheless, to unlock lupeol's complete potential, it is imperative to gain an in-depth comprehension of its structural, chemical, and pharmacological attributes.

Computational calculations of vibrational frequency, NMR, bond angles, dipole moments, and rotational constants are invaluable tools cutting across scientific disciplines [19–21]. They form the bedrock for determining molecular structures, predicting chemical reactivity, understanding properties, and facilitating critical advancements in chemistry, materials science, and pharmaceutical research. These calculations empower scientists to design drugs, materials, and catalysts with enhanced performance and tailore bond lengths, IR ties, reactivity, and behavior, impacting a diverse spectrum of fields, from foundational research to applications in environmental and materials sciences, ultimately fueling scientific progress and innovation.

This comprehensive knowledge can be acquired via computational studies, which provides valuable insights into the compound's molecular-level behavior. Computational chemistry, as a central component of our research, allows us to unravel lupeol's intricate structural and chemical properties, thus contributing to its potential in pharmaceutical development. Our research aims to comprehensively investigate lupeol, a triterpenoid compound found in the ethyl acetate leaf extract of *Justicia secunda* as reported by Bako *et al.* [11]. We conduct computational studies to provide a more detailed analysis of the isolated molecule and compare it to the experimental data, contributing to the improvement of human well-being.

2. Computational methods

The Gaussian 09 suite programs were used to carry out quantum chemical investigations on the properties of Lupeol using the HF/6-31G method and basis set as modified [22–30]. The molecular geometry of Lupeol was optimized, and vibrational frequency calculations were conducted to confirm the nature of stationary points. Subsequently, NMR calculations were performed to predict chemical shifts, using the solvent environment with the SCRF (Solvent=Ethyl Acetate) option. The obtained results were meticulously analyzed, and the optimized structure, vibrational frequencies, and calculated NMR chemical shifts were scrutinized using spectroscopic and visualization tools [31]. and compared to the experimental data. Our

findings provide valuable insights into the molecular properties of Lupeol and lay the groundworks for further exploration and understanding of its behavior in various environments.

3. Results and discussion

Comprehensive Optimization and frequency calculations were conducted on the molecule, encompassing an investigation of important structural and spectroscopic parameters [32–34]. These efforts facilitated the accurate identification and appropriate placement of the molecule within its chemical framework. Such insights are valuable for utilizing the molecule effectively in bioactivity studies and various bioassays within research endeavors.

Optimized geometry of lupeol

As shown in Figure 1, the optimized geometry of Lupeol is illustrated, providing a comprehensive representation of its molecular structure and spatial conformation [35–39]. This visualization constitutes a vital component of our computational investigation on Lupeol gotten from ethyl acetate leaf extracts of *Justicia Secunda*.

The van der Waals spheres of Lupeol molecule (Figure 2) depicts the hypothetical surfaces around each atom within the molecule, where the attractive and repulsive forces between atoms balance out. In other words, these spheres illustrate the potential spatial extent of the electron clouds surrounding each atom, accounting for van der Waals forces that arise from transient fluctuations in electron distribution. Lupeol, a triterpenoid found in various plants, exhibits these spheres to showcase the non-covalent interactions between its atoms. The spheres help visualize the molecule's three-dimensional structure and provides insights into its steric properties, influencing how Lupeol might interact with other molecules in its surroundings.

Experimental Spectra Data of the Isolated Compound (Lupeol)

NMR methods have unquestionably emerged as the predominant spectroscopic techniques for the identification and structural elucidation of natural compounds [40–44]. Therefore, the study by Bako *et al.* [11] only focused on Proton NMR for structural identification and elucidation. In the experimental proton NMR spectrum of lupeol (Figure 3), the olefinic protons of H-29 exhibited signals at δH 4.69 ppm (1H, d) and 4.58 ppm, providing evidence for the double bond between the methylene carbon (C-29) and the quaternary carbon (C-20). Additionally, the spectrum revealed the presence of seven tertiary methyl protons resonating at δ 0.75, 0.78, 0.82, 0.94, 0.96, 1.02, and 1.71 ppm, with each set of protons integrating to 3H, and displaying singlet peaks (s, CH3). Results of ^{1}H-NMR for Lupeol experimental are presented in Table A.1 as supporting information.

^{1}HNMR and ^{13}CNMR computational calculations of lupeol isolated from ethyl acetate extracts of *Justicia secunda* are shown in the Table A.2 & A.3 in the supporting information. Figure 4 shows the calculated NMR intensities.
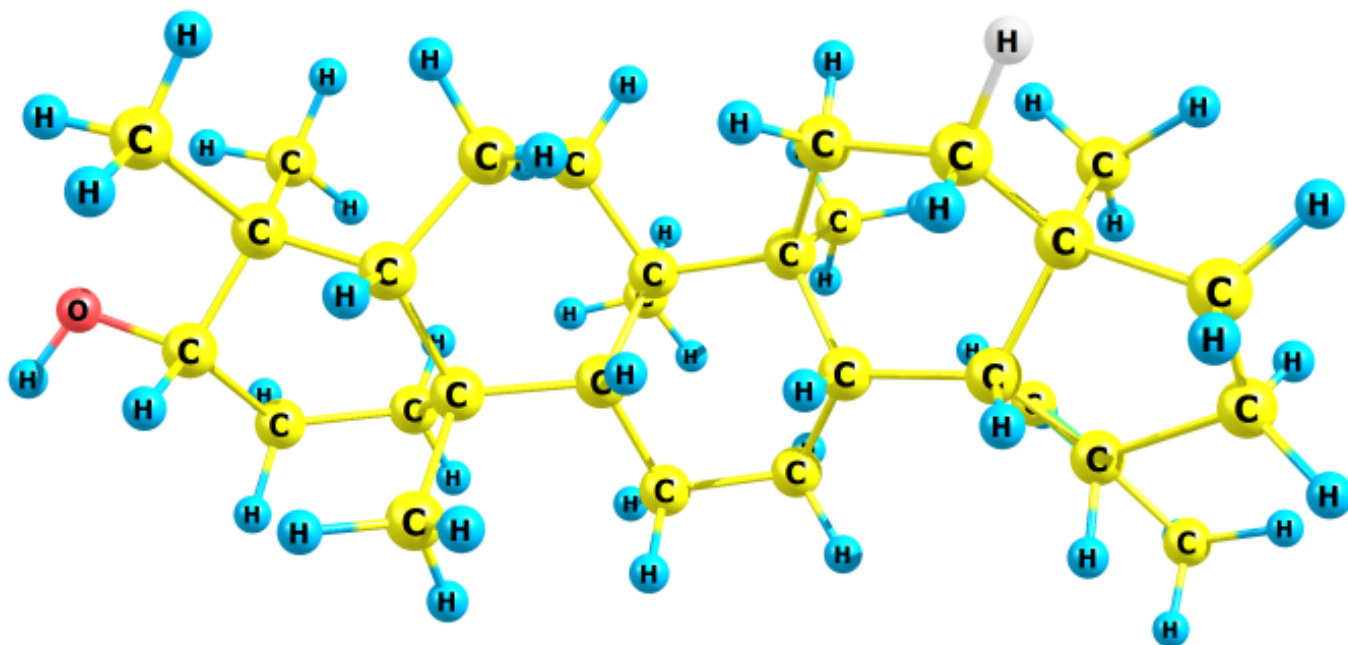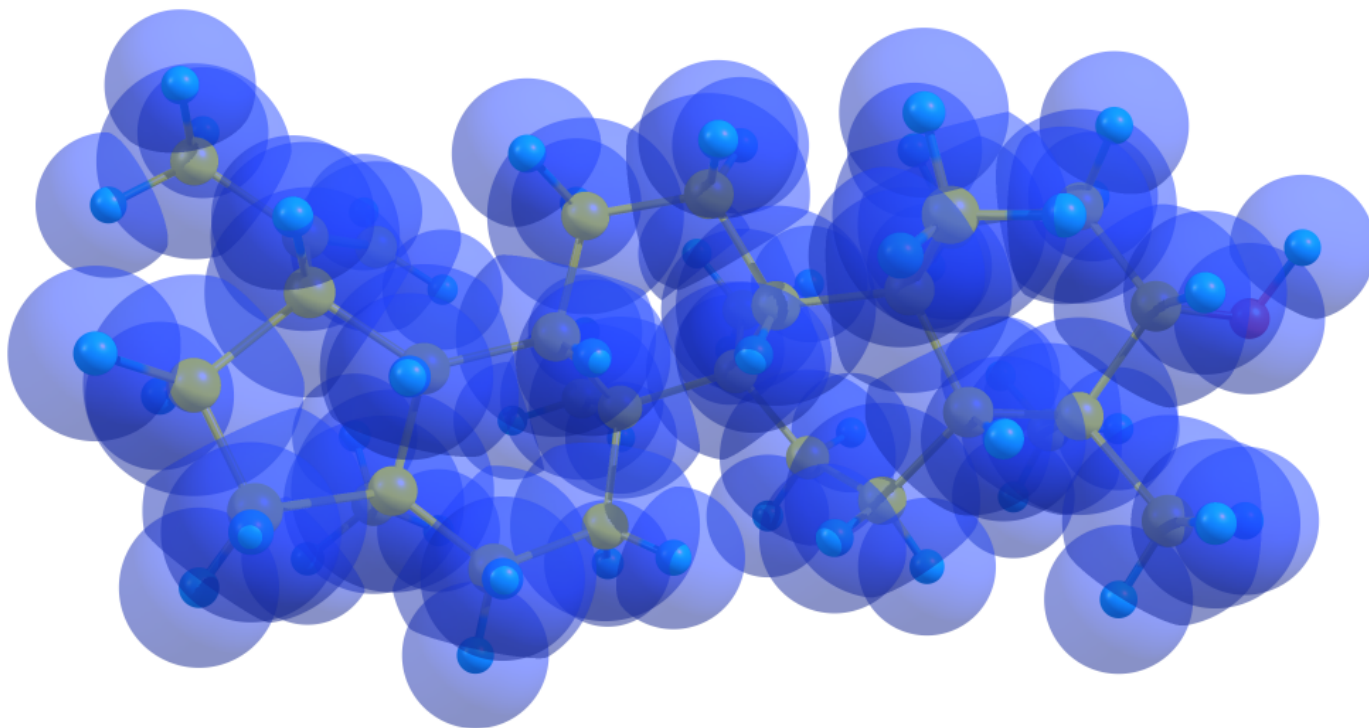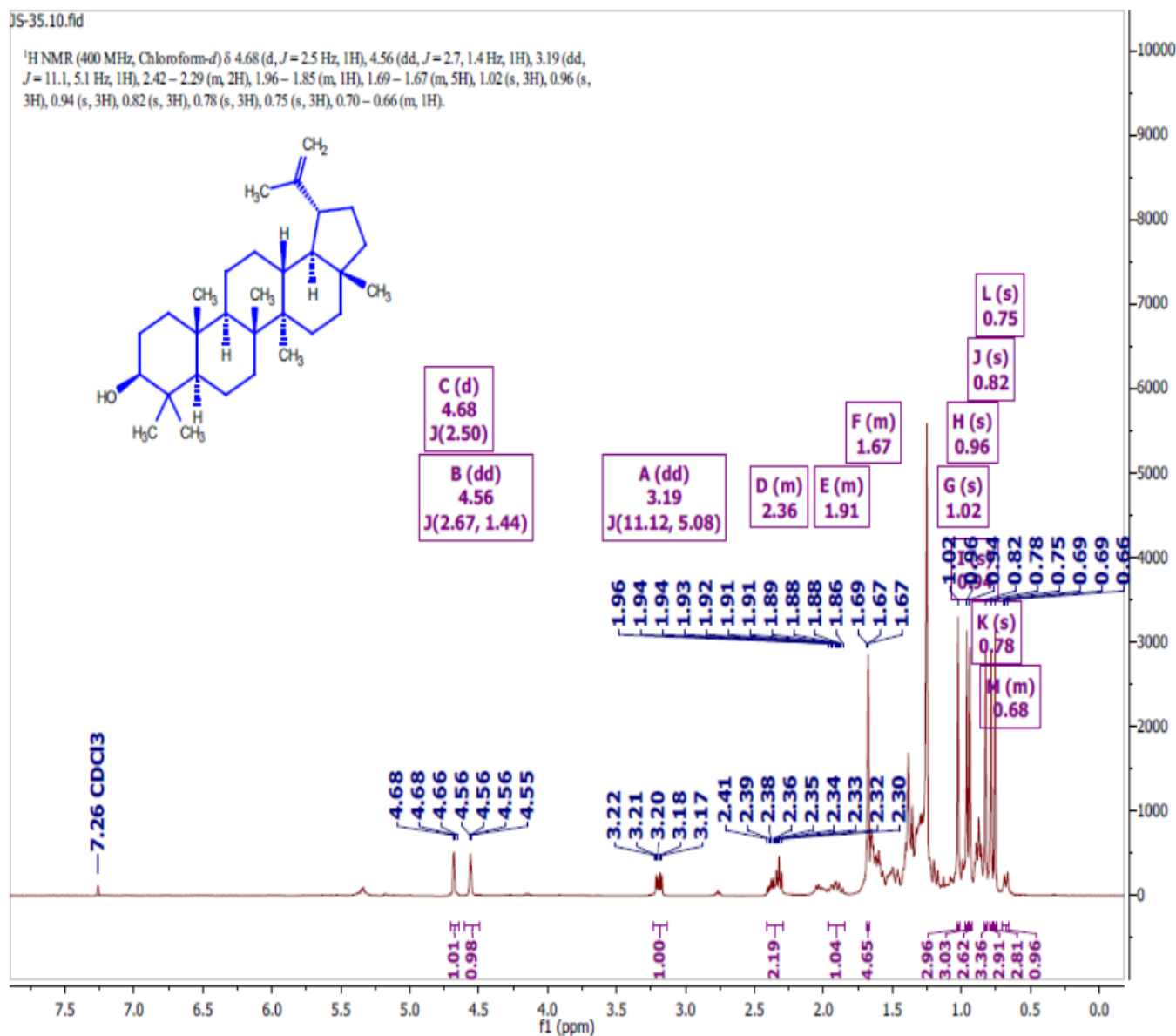
Figure 1. Optimized Geometry of Lupeol.

Figure 2. Optimized van-der waals spheres of lupeol.

The proton NMR data for optimized lupeol reveals relatively high chemical shift values (around 150-155 ppm), indicative of deshielding effects experienced by its protons, likely influenced by the presence of oxygen atoms, unsaturated bonds, or aromatic rings in the molecule. The data also suggests that certain protons share nearly identical shift values, potentially due to structural proximity or similar nearby functional groups. However, it's worthy of note that some protons have identical shift values, which are unusual in NMR spectroscopy and may warrant further investigations.

The experimental proton NMR data for Lupeol closely matches the expected features for a triterpenoid compounds,

JS-35.10.fid

¹H NMR (400 MHz, Chloroform-*d*) δ 4.68 (d, *J* = 2.5 Hz, 1H), 4.56 (dd, *J* = 2.7, 1.4 Hz, 1H), 3.19 (dd, *J* = 11.1, 5.1 Hz, 1H), 2.42 – 2.29 (m, 2H), 1.96 – 1.85 (m, 1H), 1.69 – 1.67 (m, 5H), 1.02 (s, 3H), 0.96 (s, 3H), 0.94 (s, 3H), 0.82 (s, 3H), 0.78 (s, 3H), 0.75 (s, 3H), 0.70 – 0.66 (m, 1H).

Figure 3. Experimental ¹HNMR Interpreted Spectrum of Lupeol [9].

supporting the identity of Lupeol. The presence of olefinic protons with relatively low chemical shift values is in line with the structural characteristics of Lupeol, indicating the presence of double bonds in the molecule. The presence of tertiary methyl protons in the experimental data also aligns with the calculated NMR data. Figure 5 & 6 depict the NMR Shifts and intensities of the calculated ¹HNMR.

The calculated ¹³C NMR data for Lupeol reveals a range of chemical environments within the molecule. Negative shift values, characteristic of carbon atoms in hydrocarbons and aliphatic chains, dominate the spectrum, whereas positive shift values are indicative of deshielding effects, potentially associated with carbon atoms involved in double bonds or carbonyl groups. Notably, carbon C1 serves as the reference point, with a shift value close to 0 ppm. The data also suggests the pres-

Table 1. Dipole Moment for Lupeol.

Parameter	Dipole Moment
X	-0.9702 Debye
Y	-1.3974 Debye
Z	-1.5745 Debye
Total	2.3180 Debye

ence of unique chemical environments for carbon atoms C26 and C28, likely associated with aromatic rings or other distinctive structural features. Although there are no experimental results for direct comparison, the calculated NMR data aids in understanding Lupeol's structural characteristics and the various carbon environments within the compound. Figure 7 depicts the NMR Shifts and intensities of the calculated ¹³CNMR.
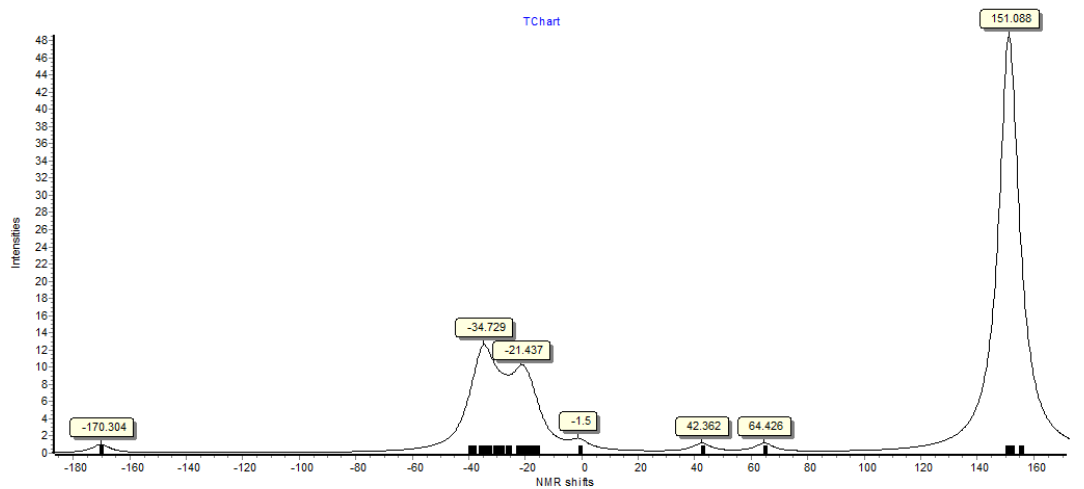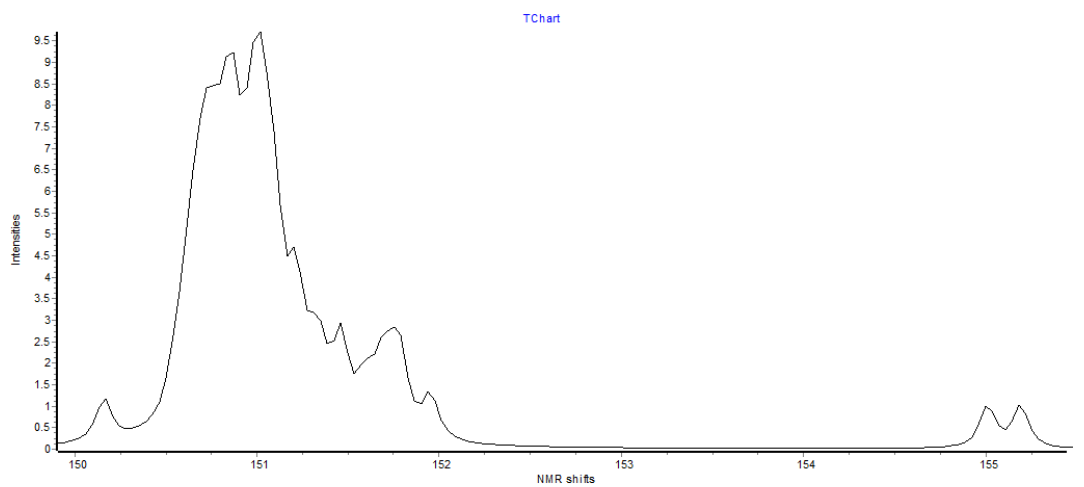
Figure 4. Calculated NMR intensities.

Figure 5. Calculated ^{1}HNMR intensities.

Vibrational frequencies

Table A.4 in the supporting information highlights the vibrational frequencies and IR intensities of Lupeol's optimized geometry using the HF/6-31G method. This data provides crucial insights into the molecular vibrations and chemical interactions within Lupeol. From Table 4, lupeol can be seen to have 237 vibrational frequencies ranging from the lowest frequency being 34.27cm^{-1} with a very low intensity at 0.103, while the highest frequency was observed at 4022.37 with a relatively high intensity of 31.77. Various intense peaks were observed, hence elucidating sharp peaks from the calculated IR intensities that can be seen in Figure 8.

Dipole Moments and Rotational Constants

Table 1 depicts the calculated dipole moments for the optimized geometry of Lupeol, employing the HF/6-31G method and basis set. These critical parameters offer essential insights into the molecular behavior and structure of Lupeol isolated
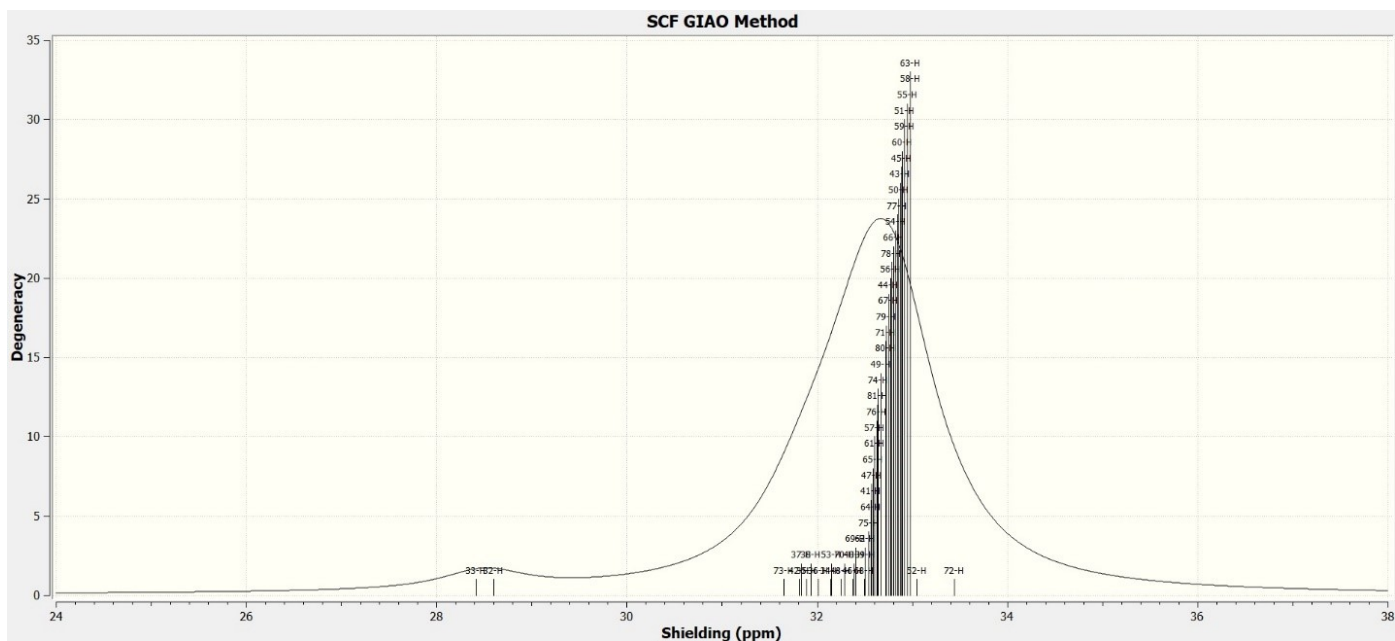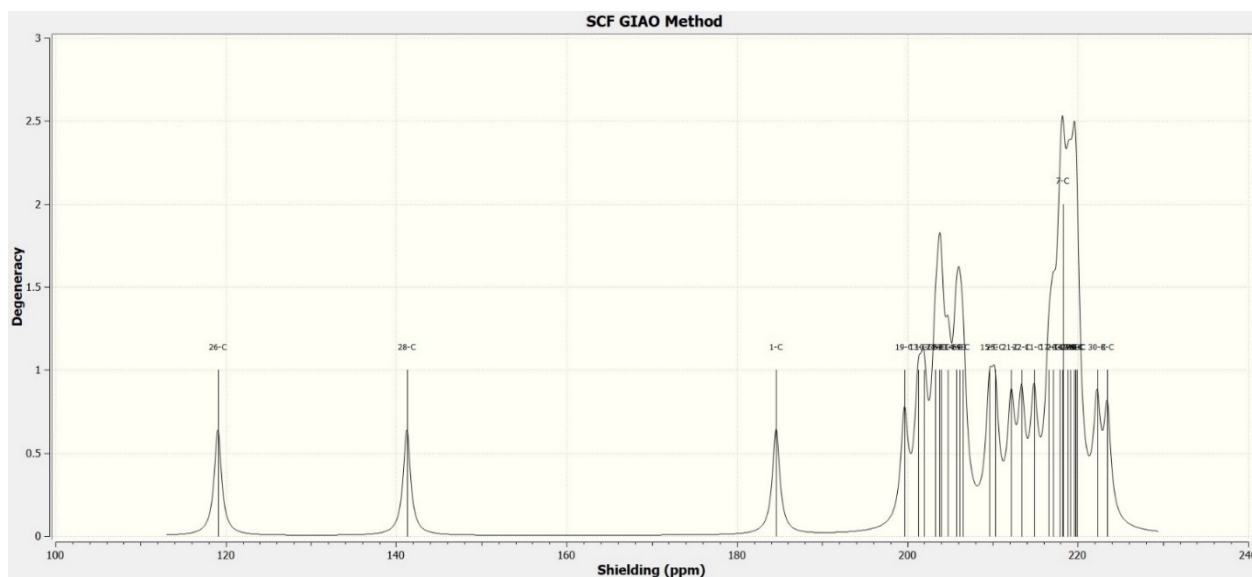
Figure 6. Calculated ^{1}HNMR intensities.

Figure 7. Calculated ^{13}CNMR intensities.

Table 2. Rotational Constants for Lupeol.

Rotational Constant	GHz
A	0.3574663
B	0.0759731
C	0.0716479

from *Justicia secunda* ethyl acetate extracts, providing a comprehensive understanding of its properties and interactions. The dipole moments describe the charge separation that occurs in the lupeol molecule. In Lupeol, the dipole moment of 2.32 Debye, as indicated in Table 1, suggests a relatively low degree of charge separation within the molecule. In terms of IR spectroscopy, this would imply that Lupeol may exhibit relatively weak IR absorption bands associated with asymmetric stretching and bending vibrations of bonds that involve significant charge separation. These vibrations typically occur in functional groups with polar bonds such as C-O, C=O, and O-H.

Rotational Constants

The rotational constants A, B, and C for lupeol represent the moments of inertia around its principal axes of rotation. From Table 2, the dipole moment A (0.3574663) is the moment of inertia around the axis with the highest value, while
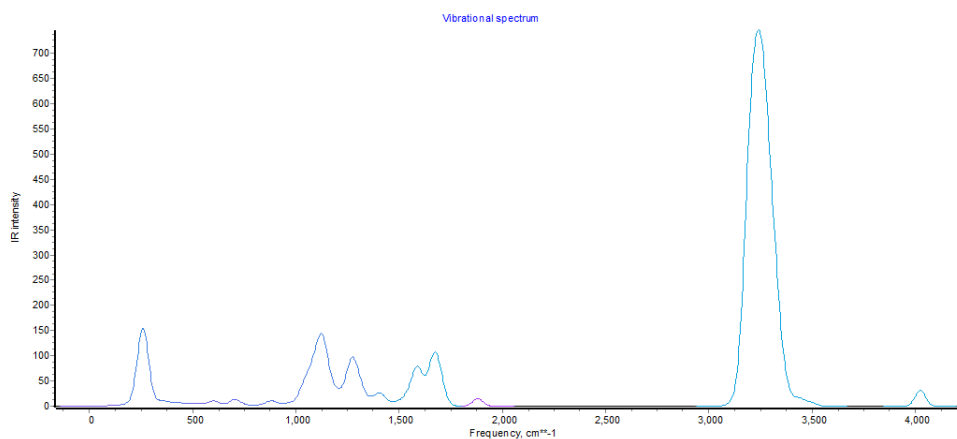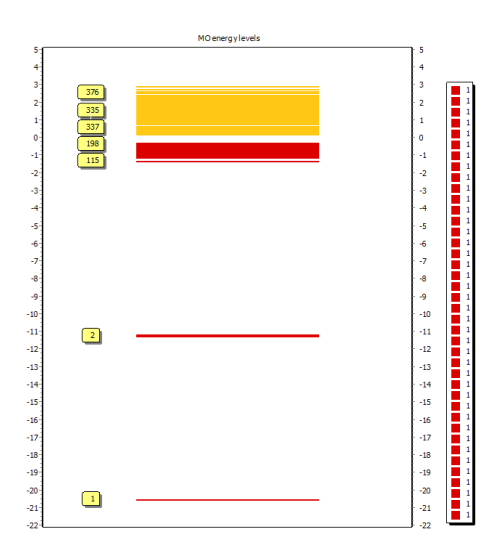
Figure 8. Calculated IR intensities of Lupeol.

Figure 9. HOMO-LUMO (Molecular Orbital Energy Levels). Keys: Red- Higher occupied molecular Orbital; Yellow- Lower unoccupied molecular Orbital.
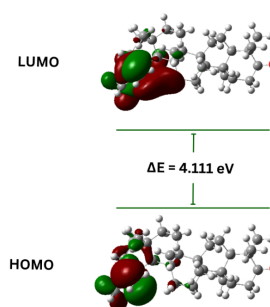

Figure 10. HOMO-LUMO Structure of Lupeol with the Band gap Energy.

This information is fundamental for various applications, such as predicting spectroscopic properties and understanding the molecule's behavior in different environments and chemical reactions [27, 45–47].

Bond Lengths and Bond Angles

Table A.5 in the supporting information, presents the calculated bond lengths and bond angles for the optimized geometry of Lupeol, using the HF/6-31G method. These data provide a comprehensive view of Lupeol's molecular structure, shedding light on the precise arrangement of its bonds and angles.

Higher Occupied Molecular Orbital and Lower Unoccupied Molecular Orbital

From Figure 9 & 10 and Table A.6 (supporting information), the higher occupied molecular orbitals are; 1, 2, 114 and 195, which have their molecular orbital energies as; -558.68, -305.96, -36.68 and -7.98ev respectively. While the Lower unoccupied molecular orbitals are; 331, 335, 371 have their molecular orbital energies as; 48.19, 16.30 and 69.27eV respectively.

C (0.0716479) corresponds to the axis with the smallest moment of inertia. These constants are crucial in understanding the molecule's rotational behavior, providing insights into its three-dimensional structure and symmetry. The specific values provided indicated the mass distribution around different axes, influencing the rotational energy levels of lupeol. A molecule with higher rotational constants along certain axes will have lower rotational energy levels in those directions.

The higher occupied molecular orbitals (HOMOs) numbered 1, 2, 114, and 195 are characterized by descending energy levels, with energies of -55 -36.68, and -7.98 eV, respectively. These values indicate a trend where the first two orbitals have significantly lower energy than orbitals 114 and 195, suggesting a varied distribution of electron density across different regions of the molecule. On the other hand, the lower unoccupied molecular orbitals (LUMOs) numbered 331, 335, and 371 exhibit ascending energy levels, with energies of 48.19, 16.30, and 69.27 eV, respectively. This arrangement provides insights into Lupeol's potential for electronic interactions, with higher energy orbitals potentially participating in reactions and bonding. The overall distribution of orbital energies signifies the molecule's electronic stability and its propensity for engaging in specific chemical processes based on these energy levels.

With a calculated band gap of 4.111 eV for lupeol, it is evident that this natural triterpene compound possesses a relatively wide band gap. This wide band gap suggests that lupeol is likely to exhibit insulating properties, requiring a substantial amount of energy to promote electrons from the highest occupied molecular orbital (HOMO) to the lowest unoccupied molecular orbital (LUMO) [48, 49].

4. Conclusion

This research represents a comprehensive computational and frequency investigation of the compound lupeol isolated from *Justicia secunda* ethyl extracts. Using quantum chemical calculations within the GAUSSIAN 09 suite of programs. Optimized geometry, IR frequencies, bond distances (R), bond angles (A), dipole moments, HOMO-LUMO, and various other molecular parameters for this isolated molecule were determined. Experimental and computational ^{1}H-NMR spectra exhibited perfect agreement, underscoring the accuracy of our calculations. This convergence opens the door to predictive applications in uncharted chemical realms, such as the design of novel drugs and materials, including the precise positioning of constituent atoms concerning their energy states, electronic charge distributions, dipoles, higher order moments, vibrational frequencies, relativistic effects, spectroscopic properties, and collision cross-sections with other molecules.

References

[1] M. Lahlou, "Screening of natural products for drug discovery", Expert opinion on drug discovery **2** (2007) 697. https://www.tandfonline.com/doi/abs/10.1517/17460441.2.5.697.

[2] E. Marsault & M. L. Peterson, "Macrocycles are great cycles: applications, opportunities, and challenges of synthetic macrocycles in drug discovery", Journal of medicinal chemistry **54** (2011) 1961. https://pubs.acs.org/doi/full/10.1021/jm1012374.

[3] C. Drahl, B. F. Cravatt & E. J. Sorensen, "Protein-reactive natural products", Angewandte Chemie International Edition **44** (2005) 5788. https://onlinelibrary.wiley.com/doi/abs/10.1002/anie.200500900.

[4] O. A. Ushie, A. C. Kendeson, B. D. Longbab, P. U. Ogofotha, S. T. Nongu, & B. Bako, "Profiling phytochemicals and antimicrobial activities of hexane and acetone crude extracts of sterculia setigera leaf", Journal of Chemical Society of Nigeria **47** (2022). https://www.journals.chemsociety.org.ng/index.php/jcsn/article/view/827.

[5] C. O. Keke, L. A. Nwaogu, C. U. Igwe, K. L. Ekeke, & W. N. Nsofor, "Phytochemical and nutritional composition of ethanol-water leaf extracts of Justicia secunda and Jatropha tanjorensis", GSC Biological and Pharmaceutical Sciences **23** (2023) 042. https://oa.mg/work/10.5281/zenodo.8260308.

[6] T. D. Locklear, *Biologically active compounds from justicia pectoralis: Significance for the treatment of dysmenorrhea*, University of Illinois at Chicago, Health Sciences Center, 2008. https://www.proquest.com/openview/e891dad92bf7edd57099372dd5ab30f5/1?pq-origsite=gscholar&cbl=18750.

[7] M. G. Ajuru, K. A. Kpekot, G. E. Robinson & M. C. Amutadi, "Proximate and phytochemical analysis of the leaves of Justicia carnea Lindi. and Justicia secunda Vahl and its taxonomic implications", J. Biomed. Biosens **2** (2022) 1. https://gpub.org/article-details.php?article-id=58.

[8] J. M. Kitadi, E. M. Lengbiye, B. Z. Gbolo, C. L. Inkoto, C. L. Muanyishay, G. L. Lufuluabo, D. S. Tshibangu, D. D. Tshilanda, B. M. Mbala, K. Ngbolua & P. T. Mpiana, "Justicia secunda Vahl species: Phytochemistry, Pharmacology and Future Directions: a mini-review", Discovery Phytomedicine **6** (2019) 157. https://biology.ejournals.ca/ejournals/phytomedicine.ejournals.ca/index.php/phytomedicine/article/view/93.

[9] A. E. Ayodele, O. I. Odusole, & A. O. Adekanmbi, "Phytochemical screening and in-vitro antibacterial activity of leaf extracts of Justicia secunda Vahl on selected clinical pathogens", MicroMedicine **8** (2020) 46. https://www.journals.tmkarpinski.com/index.php/mmed/article/view/275.

[10] B. Bako, "Applications of Justicia secunda Extracts in Functional Foods and Natural Products: A Review", Advanced Journal of Chemistry-Section B **6** (2024) 1. https://www.ajchem-b.com/article_182234.html.

[11] B. Bako, O. A. Ushie & S. P. Malu, "Lupeol and Lauric Acid Isolated from Ethyl Acetate Stem Extract of Justicia secunda and Their Antimicrobial Activity", Journal of Chemical Society of Nigeria **48** (2023) 81. https://journals.chemsociety.org.ng/index.php/jcsn/article/view/852.

[12] F. A. Macías, F. J. Mejías & J. M. Molinillo, "Recent advances in allelopathy for weed control: From knowledge to applications", Pest management science **75** (2019) 2413. https://scijournals.onlinelibrary.wiley.com/doi/abs/10.1002/ps.5355.

[13] M. Zhou, R. H. Zhang, M. Wang, G. B. Xu & S. G. Liao, "Prodrugs of triterpenoids and their derivatives", European Journal of Medicinal Chemistry **131** (2017) 222. https://www.sciencedirect.com/science/article/abs/pii/S022352341730154X.

[14] N. Zullkiflee, H. Taha & A. Usman, "Propolis: Its role and efficacy in human health and diseases", Molecules **27** (2022) 6120. https://www.mdpi.com/1420-3049/27/18/6120.

[15] A. Senthilkumar, N. Karuvantevida, L. Rastrelli, S. S. Kurup & A. J. Cheruth, "Traditional uses, pharmacological efficacy, and phytochemistry of Moringa peregrina (Forssk.) Fiori.—a review", Frontiers in pharmacology **9** (2018) 465. https://www.frontiersin.org/journals/pharmacology/articles/10.3389/fphar.2018.00465/full.

[16] A. Alam, S. Ferdosh, K. Ghafoor, A. Hakim, A. S. Juraimi, A. Khatib & Z. I. Sarker, "Clinacanthus nutans: A review of the medicinal uses, pharmacology and phytochemistry", Asian Pacific journal of tropical medicine **9** (2016) 402. https://www.sciencedirect.com/science/article/pii/S1995764516300116.

[17] J. A. Keith, V. Vassilev-Galindo, B. Cheng, S. Chmiela, M. Gastegger, K. R. Mu¨ller & A. Tkatchenko, "Combining machine learning and computational chemistry for predictive insights into chemical systems", Chemical reviews **121** (2021) 9816. https://pubs.acs.org/doi/full/10.1021/acs.chemrev.1c00107.

[18] G. O. Izuagbe, E. O. Emmanuella, L. Hitler, M. K. Emmanuel, E. E. Emmanuel, O. E. Henry, J. I. Onyinye, P. O. Amoawe & O. Faith, "Antibacterial potential of N-(2-furylmethylidene)-1, 3, 4-thiadiazole-2-amine: Experimental and theoretical investigations", Journal of the Indian Chemical Society **99** (2022) 100597. https://www.sciencedirect.com/science/article/abs/pii/S001945222200259X.

[19] E. G. Lewars, *Computational chemistry: Introduction to the theory and applications of molecular and quantum mechanics*, Springer Cham, 2011, pp. 318–728. https://link.springer.com/book/10.1007/978-3-319-30916-3.

[20] M. Biczysko, J. Bloino, G. Brancato, I. Cacelli, C. Cappelli, A. Ferretti, A. Lami, S. Monti, A. Pedone, G. Prampolini, C. Puzzarini, F. Santoro, F. Trani & G. Villani, "Integrated computational approaches for spectro-

scopic studies of molecular systems in the gas phase and in solution: pyrimidine as a test case", Theoretical Chemistry Accounts **131** (2012) 1. https://link.springer.com/article/10.1007/s00214-012-1201-3.

[21] G. O. Izuagbe, L. Hitler, M. K. Emmanuel, E. E. Emmanuel, E. O. Emmanuella, P. O. Amoawe, O. E. Henry & O. Faith, "Antibacterial Potential of 2-(-(2-Hydroxyphenyl)-methylidene)-amino)nicotinic Acid: Experimental, DFT Studies, and Molecular Docking Approach", Appl Biochem Biotechnol **194** (2022) 5680. https://link.springer.com/article/10.1007/s12010-022-04054-9.

[22] Y. Ma, J. Xiong, P. Zhang, Y. Li, S. Zhang, Z. Wang, L. Xu, H. Guo, K. Chen & Y. Wei, "Recent Progress on Density Functional Theory Calculations for Catalytic Control of Air Pollution", *ACS ES&T Engineering* **4** (2023) 47. https://pubs.acs.org/doi/abs/10.1021/acsestengg.3c00208.

[23] J. S. Costa, C. B. R. D. Santos, K. S. L. Costa, R. D. S. Ramos, C. H. T. D. P. D. Silva & W. J. D. C. Macêdo, "Validation of computational methods applied in molecular modeling of caffeine with epithelial anticancer activity: Theoretical study of geometric, thermochemical and spectrometric data", Química Nova **41** (2018) 553. https://www.scielo.br/j/qn/a/6L6hSvdgT7yZFxsbPs4gwnD/?format=html&lang=en.

[24] M. E. Khan, E. E. Etim, V. J. Anyam, A. Abel, I. G. Osigbemhe, & C. T. Agber, "Computational studies on Emodin (C15H10O5) from Methanol extract of Pteridium acquilinum leaves", J. Nig. Soc. Phys. Sci. **3** (2021) 360. https://www.journal.nsps.org.ng/index.php/jnsps/article/view/301.

[25] I. G. Osigbemhe, H. Louis, E. M. Khan, E. E. Etim, D. O. Odey, A. P. Oviawe, H. O. Edet & F. Obuye, "Synthesis, characterization, DFT studies, and molecular modeling of 2-(-(2-hydroxy-5-methoxyphenyl)-methylidene)-amino) nicotinic acid against some selected bacterial receptors", Journal of the Iranian Chemical Society **19** (2022) 3561. https://link.springer.com/article/10.1007/s13738-022-02550-7.

[26] M. J. Frisch, G. W. Trucks, H. B. Schlegel, G. E. Scuseria, M. A. Robb, J. R. Cheeseman, G. Scalmani, V. Barone, B. Mennucci, G. A. Petersson, H. Nakatsuji, M. Caricato, X. Li, H. P. Hratchian, A. F. Izmaylov, J. Bloino, G. Zheng, J. L. Sonnenberg, M. Hada, M. Ehara, K. Toyota, R. Fukuda, J. Hasegawa, M. Ishida, T. Nakajima, Y. Honda, O. Kitao, H. Nakai, T. Vreven, J. A. Montgomery Jr., J. E. Peralta, F. Ogliaro, M. Bearpark, J. J. Heyd, E. Brothers, K. N. Kudin, V. N. Staroverov, R. Kobayash, J. Normand, K. Raghavachari, A. Rendell, J. C. Burant, S. S. Iyengar, J. Tomasi, M. Cossi, N. Rega, J. M. Millam, M. Klene, J. E. Knox, J. B. Cross, V. Bakken, C. Adamo, J. Jaramillo, R. Gomperts, R. E. Stratmann, O. Yazyev, A. J. Austin, R. Cammi, C. Pomelli, J. W. Ochterski, R. L. Martin, K. Morokuma, V. G. Zakrzewski, G. A. Voth, P. Salvador, J. J. Dannenberg, S. Dapprich, A. D. Daniels, O. Farkas, J. B. Foresman, J. V. Ortiz, J. Cioslowski & D. J. Fox, "Gaussian 09, Revision D. 01, Gaussian", Inc. Wallingford CT (2009). https://cir.nii.ac.jp/crid/1370298757422456580.

[27] E. E. Etim, A. I. Onen, C. Andrew, U. Lawal, I. S. Udegbunam & O. A. Ushie, "Computational Studies of C5H5N Isomers", Journal of Chemical Society of Nigeria, **43** (2018). https://journals.chemsociety.org.ng/index.php/jcsn/article/view/154.

[28] C. Andrew, E. E. Etim, O. A. Ushie & G. P. Khanal, "Vibrational-Rotational Spectra of Normal Acetylene and Doubly Deuterated Acetylene: Experimental and Computational Studies", Chemical Science **7** (2018) 77. chrome-extension://efaidnbmnnnibpcajpcglclefindmkaj/http://www.e-journals.in/pdf/V7N1/77-82.pdf.

[29] E. E. Etim, G. E. Oko, A. I. Onen, O. A. Ushie, U. Lawal & G. P. Khanal, "Computational Studies of Sulphur trioxide (SO3) and its protonated analogues", Journal of Chemical Society of Nigeria **43** (2018). https://journals.chemsociety.org.ng/index.php/jcsn/article/view/153.

[30] E. E. Etim, B. S. Abah, I. E. Mbakara, E. J. Inyang & O. P. Ukafia, "Quantum Chemical Calculations on Silicon Monoxide (SiO) and its Protonated Analogues", Tropical Journal of Applied Natural Sciences **2** (2017) 61. https://www.researchgate.net/publication/330555369_Quantum_Chemical_Calculations_on_Silicon_Monoxide_SiO_and_its_Protonated_Analogues.

[31] E. E. Etim, S. A. Olagboye, O. E. Godwin & I. M. Atiatah, "Quantum Chemical studies on Silicon tetrafluoride and its protonated analogues", International Journal of Modern Chemistry **12** (2020) 26. chrome-extension://efaidnbmnnnibpcajpcglclefindmkaj/https://www.researchgate.net/profile/Oko-Emmanuel-Godwin-2/publication/347553285_Share_'2020_SiF4_Published_paper/links/5fe1a9a192851c13fead9027/Share-2020-SiF4-Published-paper.pdf.

[32] E. E. Etim, E. Oko, Godwin, I. F. Sambo & S. A. Olag-

boye, "Quantum Chemical Studies on Furan and Its Isomers", International Journal of Modern Chemistry **12** (2020) 77. chrome-extension://efaidnbmnnnibpcajpcglclefindmkaj/https://www.researchgate.net/profile/Oko-Emmanuel-Godwin-2/publication/347553041_Quantum_Chemical_studies_of_Furan/links/5fe1a94b45851553a0df5889/Quantum-Chemical-studies-of-Furan.pdf.

[33] E. E. Etim, G. E. Oko, A. I. Onen, O. A. Ushie, C. Andrew, U. Lawal & G. P. Khanal, "Computational Studies of Sulphur Trioxide (SO3) and its Protonated Analogues", J. Chem Soc. Nigeria **43** (2018) 10. https://journals.chemsociety.org.ng/index.php/jcsn/article/view/153.

[34] E. E. Etim, B. S. Abah, I. E. Mbakara, E. J. Inyang, O. P. Ukafia, "Quantum Chemical Calculations on Silicon Monoxide (SiO) and its Protonated Analogues", Trop. J. Appl. Nat. Sci. **2** (2017) 61. https://www.researchgate.net/publication/330555369_Quantum_Chemical_Calculations_on_Silicon_Monoxide_SiO_and_its_Protonated_Analogues.

[35] J. P. Shinggu, E. E. Etim, & A. I. Onen, "Quantum Chemical Studies on C2H2O Isomeric Species: Astrophysical Implications, and Comparison of Methods", Communication in Physical Sciences **9** (2023). https://journalcps.com/index.php/volumes/article/view/349.

[36] J. P. Shinggu, E. E. Etim & A. I. Onen, "Protonation-Induced Structural and Spectroscopic Variations in Molecular Species: A Computational Study on N2, H2, CO, CS, and PH3", Communication in Physical Sciences **9** (2023). https://journalcps.com/index.php/volumes/article/view/388.

[37] J. P. Shinggu, E. E. Etim & A. I. Onen, "Isotopic Effects on the Structure and Spectroscopy of Thioformaldehyde, Dihydrogen and Water", Advanced. Journal of Chemistry. A **6** (2023) 366. https://www.ajchem-a.com/article_178011.html.

[38] E. E. Etim, E. G. Oko, I. Fridy & A. Olagboye, "Quantum Chemical Studies on Furan and Its Isomers", International Journal of Modern Chemistry **12** (2020) 77. https://www.researchgate.net/publication/347553041_Quantum_Chemical_studies_of_Furan.

[39] D. Alahira, J. P. Shinggu & B. Bako, "Quantum chemical and molecular docking studies of luteolin and naringerin found in tigernut: A study of their anti-cancer properties", Journal of Medicinal and Nanomaterials Chemistry **6** (2024) 64. chrome-extension://efaidnbmnnnibpcajpcglclefindmkaj/https://jmnc.samipubco.com/article_194115_4eada3e6dc19ae7a70a8946cd686ae36.pdf.

[40] O. A. Ushie, E. E Etim, A. I. Onen, C. Andrew, U. Lawal & G. P. Khanal, "Computational Studies of β-amyrin acetate (C32H52O2) Detected in Methanol Leaf Extract of Chrysophyllum albidium", Journal of Chemical Society of Nigeria **44** (2019) 561. https://www.journals.chemsociety.org.ng/index.php/jcsn/article/view/305.

[41] I. Jantan, S. N. A. Bukhari, M. A. S. Mohamed, L. K. Wai & M. A. Mesaik, "The evolving role of natural products from the tropical rainforests as a replenishable source of new drug leads", Drug Discovery and Development-From Molecules to Medicine (2015) 3. https://www.intechopen.com/chapters/47844.

[42] M. E. Khan, C. E. Elum, A. O. Ijeomah, P. J. Ameji, I. G. Osigbemhe, E. E. Etim, J. V. Anyam, A. Abel, & C. T. Agber, "Isolation, Characterization, Antimicrobial and Theoretical Investigation of Some Bioactive Compounds Obtained from the Bulbs of Calotropisprocera", Journal of the Nigerian Society of Physical Sciences **5** (2023) 1576. https://doi.org/10.46481/jnsps.2023.1576.

[43] I. G. Osigbemhe, E. E. Oyoita, H. Louis, E. M. Khan, E. E. Etim, H. O. Edet, O. J. Ikenyirimba, A. P. Oviawe & F. Obuye, "Antibacterial potential of N-(2-furylmethylidene)-1, 3, 4-thiadiazole-2-amine: Experimental and theoretical investigations", Journal of Molecular Structure **1253** (2023) 131408. https://www.sciencedirect.com/science/article/abs/pii/S001945222200259X.

[44] E. G. Oko, A. E. Peter & E. E. Emmanuel, "Phytochemical and Antimicrobial Properties of African Peach (*Sarcocephalus Latifolius*)", Organic & Medicinal Chem IJ. **9** (2020) 555775. https://ideas.repec.org/a/adp/jomcij/v9y2020i5p198-204.html.

[45] E. E. Etim, J. E. Asuquo, O. C. Ngana & G. O. Ogofotha, "Investigation on the thermochemistry, molecular spectroscopy and structural parameters of pyrrole and its isomers: a quantum chemistry approach", Journal of Chemical Society of Nigeria **47** (2022). https://journals.chemsociety.org.ng/index.php/jcsn/article/view/704.

[46] E. E. Etim, M. E. Khan, O. E. Godwin & G. O. Ogofotha, "Quantum Chemical Studies on C4H4N2 Isomeric Molecular Species", Journal

of the Nigerian Society of Physical Sciences (2021) 429. https://www. journal.nsps.org.ng/index.php/jnsps/article/view/282.

[47] E. E. Etim, E. G. Oko, I. F. Sambo & S. Adeoye, "Suspected Error in Some Experimentally Reported Proton Affinity Values: Insight from Quantum Chemical Calculations", Int. J. Modern Anal. Sep. Sci, *8*(1) (2020) 28. https://www.researchgate.net/publication/347551664_Suspected_Error_in_Some_Experimentally_Reported_Proton_Affinity_Values_Insight_from_Quantum_Chemical_Calculations.

[48] E. E. Etim, S. A. Olagboye, O. E. Godwin & I. M. Atiatah, "Quantum Chemical studies on Silicon tetrafluoride and its protonated analogues", Int. J. Modern Chem **12** (2020) 26. https://www.researchgate.net/publication/347553285_Share_%272020_SiF4_Published_paper.

[49] A. I. Onen, J. Joseph, E. Etim & N. O. Eddy, "Quantum Chemical Studies on the Inhibition Mechanism of Ficus carica, FC and Vitellaria paradoxa, VP Leaf Extracts", Journal of Advanced Chemical Sciences **3** (2017) 496. https://www.semanticscholar.org/paper/Quantum-Chemical-Studies-on-the-Inhibition-of-Ficus-Onen-Joseph/be9a0dfc0a1e07a733793a8574adda0a17be0cb5.

APPENDIX A.

Table A.1. Experimental ^{1}HNMR Spectra Data of Lupeol [12]

Position of Proton (H)	Experimental ^{1}H Chemical shift $\mathbf{\delta}$ (ppm), J (Hz)
1	-
2	1.67, m
3	3.19, m
4	-
5	0.68, m
6	-
7	-
8	-
9	-
10	-
11	-
12	-
13	-
14	-
15	-
16	-
17	-
18	-
19	2.36, m
20	-
21	-
22	-
23	0.96, s
24	0.75, s
25	0.82, s
26	1.02, s
27	0.94, s
28	0.78, s
29	4.68, d
	4.56, dd
30	1.91, m

Table A.2. Calculated ^{1}HNMR Shifts and Intensities (HF/6-31G)

Proton (H) Positions	NMR Shifts	Intensity
H1	155.0062	1
H2	155.19	1
H3	151.4619	1
H3	151.7143	1
H4	151.5869	1
H5	151.7689	1
H6	151.667	1
H7	151.1003	1
H8	151.2108	1
H9	151.0376	1
H10	151.7859	1
H11	150.7258	1
H12	150.8493	1
H13	150.7147	1
H14	151.2285	1
H15	151.0298	1
H16	151.3493	1
H17	150.9264	1
H18	150.745	1
H19	150.678	1
H20	150.5494	1
H21	151.4505	1
H22	150.774	1
H23	150.6484	1
H24	150.826	1
H25	150.9936	1
H26	150.6166	1
H27	150.678	1
H28	150.7038	1
H29	150.9978	1
H30	151.0984	1
H31	150.6166	1
H32	151.0389	1
H33	151.0141	1
H34	150.7984	1
H35	150.8505	1
H36	151.1042	1
H37	151.1946	1
H38	151.3096	1
H39	150.8793	1
H40	150.1559	1
H41	151.9492	1
H42	150.9593	1
H43	151.058	1
H44	150.9723	1
H45	150.7594	1
H46	150.8234	1
H47	150.8723	1
H48	150.8828	1
H49	150.9656	1

Table A.3. Calculated ^{13}CNMR Shifts and Intensities (HF/6-31G)

Carbon (C) Positions	NMR Shifts	Intensity
C1	-0.99370000	1
C2	-33.5193	1
C3	-34.2821	1
C4	-22.1261	1
C5	-20.1514	1
C6	-22.5142	1
C7	-34.6418	1
C8	-39.8709	1
C9	-22.9535	1
C10	-18.3348	1
C11	-31.2666	1
C12	-35.2191	1
C13	-17.6819	1
C14	-34.5975	1
C15	-26.0337	1
C16	-35.9879	1
C17	-33.0091	1
C18	-36.311	1
C19	-16.0533	1
C20	-20.3598	1
C21	-28.5832	1
C22	-29.8028	1
C23	-21.1833	1
C24	-19.6722	1
C24	-26.6967	1
C26	64.5305	1
C27	-35.5094	1
C28	42.3449	1
C29	-36.1233	1
C30	-38.6698	1

Table A.4. Calculated Vibrational frequencies and IR Intensities

Frequency (cm^{-1})	IR Intensity
34.2664	0.103
48.5397	0.034
64.9959	0.0374
74.5675	0.1218
95.6402	0.5599
109.7831	0.0353
122.9271	0.4645
133.5016	0.7972
159.058	0.4743
179.0287	0.8137
180.8244	1.1814
191.7638	1.6467
198.5778	0.5301
200.2592	0.0625
205.7251	0.1482
234.1184	15.6098
238.3642	2.8351
250.3291	0.2801
257.5912	134.1213
270.3491	5.226
279.5448	0.4498
283.666	1.769
287.6795	3.7178
293.0775	1.9557
305.1297	0.0752
308.4898	0.4929
314.4236	0.1673
316.2735	0.3221
335.6664	0.2081
340.6585	1.9832
347.8063	6.1192
363.1674	0.5909
367.6254	0.1677
377.4335	0.6758
384.3601	1.6566
394.6771	2.6703
404.6349	0.0203
415.7407	0.568
423.5642	0.4645
444.4364	3.0956
445.9229	1.5534
475.5432	0.4778
485.7342	0.9767
498.3908	0.6236
502.1873	0.5731
513.838	3.0382
521.5359	0.1888
529.2357	1.2657
556.1511	0.7178
566.7736	0.0299
579.3761	1.6167
594.7113	4.1184
608.1828	5.0873
611.9556	0.119
629.1391	0.8746
679.9742	0.4094
692.4149	1.2301
698.0177	10.6065
729.4774	2.2854
734.8164	1.095
752.4131	0.5169
775.297	0.1029
797.6294	0.4945
811.7264	0.491
822.5956	0.803
857.7038	1.679
864.7266	2.2562
875.4045	0.6138
881.8408	5.5482
893.5278	0.9111
910.4034	1.2041
927.7776	0.5442
938.2776	0.713
961.5413	4.467

974.4943	0.2542	1410.288	1.8963
982.122	0.1434	1411.7944	5.8833
999.8035	2.7213	1412.5977	1.2015
1009.8951	1.3765	1425.0494	4.0427
1018.2245	0.2185	1442.5598	1.5517
1027.8411	0.7023	1461.999	0.78
1033.9286	6.0052	1471.5398	1.283
1035.0279	14.3456	1486.2445	0.1284
1041.6659	3.5362	1487.0182	1.9725
1048.6255	1.6696	1495.0898	0.8008
1052.4703	14.7286	1503.3857	2.4188
1064.638	12.0711	1508.291	0.1224
1073.2384	0.6046	1512.892	2.2713
1079.0657	1.6119	1515.6132	0.5326
1088.8747	1.9662	1524.8931	0.3805
1092.2938	24.7727	1525.5287	0.46
1092.9557	31.4288	1528.5183	0.1989
1101.4615	2.3848	1537.536	6.9604
1118.1683	2.2633	1540.0626	1.7197
1125.4265	12.5059	1544.3392	1.1979
1128.9733	87.9846	1547.2054	1.0391
1135.1578	4.3467	1559.9814	2.4595
1138.199	1.229	1564.7342	0.1102
1143.1725	4.1059	1565.4302	10.7325
1161.5519	2.2199	1568.0011	1.6676
1164.7138	0.2517	1578.1227	3.7951
1168.3107	15.4217	1581.8366	8.1829
1181.0978	1.2439	1584.5031	9.8351
1183.4637	2.4076	1588.3975	7.3871
1199.7338	8.0952	1591.3691	20.4861
1203.7328	6.138	1595.0816	16.9691
1216.6105	5.2351	1607.9255	1.158
1222.452	0.9235	1642.0268	4.0862
1226.5607	0.85	1644.3175	9.8725
1244.5387	0.9188	1647.4254	0.2473
1258.382	14.4675	1652.3138	2.0329
1259.2886	21.631	1653.7271	0.9103
1264.8355	11.0289	1655.0138	6.2493
1276.3025	40.0859	1655.2165	5.8388
1282.3415	3.3559	1656.9377	4.2932
1299.0668	1.5954	1659.1451	2.4512
1307.479	25.768	1661.9595	1.8695
1319.0329	0.6775	1663.7721	6.4165
1320.7218	1.2198	1665.3028	9.3185
1328.8212	1.4806	1666.6763	4.8188
1343.1829	1.924	1668.4273	2.3947
1354.1874	3.4833	1671.5672	8.5781
1358.8548	0.6519	1672.8819	0.5894
1369.4395	0.1122	1674.9083	6.439
1372.8993	0.1679	1678.1501	1.8924
1376.2425	3.5577	1679.1135	9.8012
1391.2007	4.5473	1680.7766	3.107
1396.5452	5.6622	1683.5313	8.1437
1404.6947	2.1273		

1687.506	0.3813
1692.5979	18.9101
1697.121	5.0813
1698.0846	6.2274
1723.7758	4.0301
1878.4644	15.1766
3114.4921	8.0212
3156.965	18.4959
3165.5629	6.2208
3166.3274	33.5819
3179.0947	38.4578
3179.9989	35.004
3181.9261	13.0747
3188.4155	21.8916
3192.1955	31.5924
3194.2028	5.3689
3195.0516	50.2462
3199.0491	55.291
3201.1393	36.6022
3204.8758	13.9607
3206.5073	27.9674
3213.7359	46.8039
3214.0439	40.0394
3215.1071	34.7092
3216.2642	0.4769
3220.3914	3.8766
3224.5676	115.0688
3227.4334	32.2797
3232.5263	20.5689
3234.4275	46.5231
3235.4988	33.4462
3241.7579	28.9395
3243.4694	50.1792
3244.4624	18.7824
3246.9113	10.1243
3255.1906	62.2547
3259.2406	69.7346
3261.9126	64.9835
3265.7863	66.9811
3271.6732	73.6524
3273.0942	37.1242
3277.4299	36.2298
3287.1829	40.0703
3297.2231	29.657
3298.2179	42.4032
3303.465	21.3698
3304.9603	31.0005
3309.0543	23.6702
3316.329	42.4452
3320.1686	21.9835
3327.9026	56.752
3338.8346	25.7311
3370.623	33.1197
3434.9867	15.4369
3492.1246	7.4925
4022.3717	31.7654

Table A.5. Calculated Bond Lengths and Bond Angles of Lupeol

Parameter	Predicted Value
R(1-2)	1.536
R(1-6)	1.539
R(1-31)	1.443
R(1-73)	1.084
R(2-3)	1.540
R(2-74)	1.084
R(2-75)	1.086
R(3-4)	1.543
R(3-76)	1.075
R(3-77)	1.084
R(4-5)	1.588
R(4-9)	1.580
R(4-17)	1.554
R(5-6)	1.581
R(5-12)	1.548
R(5-81)	1.086
R(6-7)	1.545
R(6-8)	1.544
R(7-69)	1.084
R(7-70)	1.081
R(7-71)	1.086
R(8-66)	1.083
R(8-67)	1.080
R(8-68)	1.081
R(9-10)	1.564
R(9-14)	1.552
R(9-61)	1.084
R(10-11)	1.557
R(10-13)	1.644
R(10-18)	1.554
R(11-12)	1.533
R(11-62)	1.084
R(11-63)	1.082
R(12-64)	1.083
R(12-65)	1.083
R(13-15)	1.560
R(13-22)	1.579
R(13-30)	1.541
R(14-16)	1.557
R(14-56)	1.083
R(14-57)	1.083
R(15-16)	1.530
R(15-19)	1.570
R(15-53)	1.080
R(16-54)	1.085
R(16-55)	1.082
R(17-78)	1.085
R(17-79)	1.080
R(17-80)	1.083
R(18-58)	1.079
R(18-59)	1.076
R(18-60)	1.081
R(19-20)	1.560

R(19-24)	1.563	A(76-3-77)	106.5
R(19-42)	1.087	A(5-4-9)	109.5
R(20-21)	1.534	A(5-4-17)	107.9
R(20-23)	1.549	A(4-5-6)	116.0
R(20-29)	1.553	A(4-5-12)	112.9
R(21-22)	1.567	A(4-5-81)	104.8
R(21-46)	1.087	A(9-4-17)	105.9
R(21-47)	1.088	A(4-9-10)	118.5
R(22-48)	1.079	A(4-9-14)	114.5
R(22-49)	1.085	A(4-9-61)	100.8
R(23-25)	1.553	A(4-17-78)	110.7
R(23-40)	1.086	A(4-17-79)	111.9
R(23-41)	1.083	A(4-17-80)	111.6
R(24-25)	1.581	A(6-5-12)	112.9
R(24-26)	1.518	A(6-5-81)	103.6
R(24-37)	1.088	A(5-6-7)	108.0
R(25-38)	1.083	A(5-6-8)	115.6
R(25-39)	1.083	A(12-5-81)	105.2
R(26-27)	1.514	A(5-12-11)	114.8
R(26-28)	1.325	A(5-12-64)	108.0
R(27-34)	1.087	A(5-12-65)	109.8
R(27-35)	1.082	A(7-6-8)	107.1
R(27-36)	1.085	A(6-7-69)	111.3
R(28-32)	1.066	A(6-7-70)	110.2
R(28-33)	1.074	A(6-7-71)	111.0
R(29-43)	1.080	A(6-8-66)	110.9
R(29-44)	1.078	A(6-8-67)	113.5
R(29-45)	1.085	A(6-8-68)	108.8
R(30-50)	1.070	A(69-7-70)	108.3
R(30-51)	1.077	A(69-7-71)	107.8
R(30-52)	1.085	A(70-7-71)	108.1
R(31-72)	0.951	A(66-8-67)	107.8
A(2-1-6)	113.9	A(66-8-68)	107.9
A(2-1-31)	110.2	A(67-8-68)	107.6
A(2-1-73)	109.8	A(10-9-14)	109.6
A(1-2-3)	114.0	A(10-9-61)	105.3
A(1-2-74)	107.6	A(9-10-11)	108.9
A(1-2-75)	109.2	A(9-10-13)	108.7
A(6-1-31)	108.0	A(9-10-18)	110.2
A(6-1-73)	107.3	A(14-9-61)	106.5
A(1-6-5)	108.1	A(9-14-16)	112.6
A(1-6-7)	107.8	A(9-14-56)	110.6
A(1-6-8)	109.9	A(9-14-57)	109.0
A(31-1-73)	107.3	A(11-10-13)	112.9
A(1-31-72)	113.1	A(11-10-18)	105.8
A(3-2-74)	108.7	A(10-11-12)	114.3
A(3-2-75)	110.4	A(10-11-62)	110.6
A(2-3-4)	113.2	A(10-11-63)	108.4
A(2-3-76)	107.8	A(13-10-18)	110.3
A(2-3-77)	109.1	A(10-13-15)	108.4
A(74-2-75)	106.6	A(10-13-22)	113.6
A(4-3-76)	109.9	A(10-13-30)	107.8
A(4-3-77)	110.1	A(10-18-58)	113.9
A(3-4-5)	110.2	A(10-18-59)	110.3
A(3-4-9)	115.4	A(10-18-60)	110.9
A(3-4-17)	107.7	A(12-11-62)	109.6

A(12-11-63)	108.1
A(11-12-64)	109.8
A(11-12-65)	108.9
A(62-11-63)	105.3
A(64-12-65)	105.2
A(15-13-22)	105.9
A(15-13-30)	113.5
A(13-15-16)	112.6
A(13-15-19)	117.5
A(13-15-53)	102.0
A(22-13-30)	107.7
A(13-22-21)	117.8
A(13-22-48)	110.1
A(13-22-49)	108.4
A(13-30-50)	111.6
A(13-30-51)	112.9
A(13-30-52)	110.2
A(16-14-56)	109.9
A(16-14-57)	108.1
A(14-16-15)	108.8
A(14-16-54)	109.1
A(14-16-55)	111.6
A(56-14-57)	106.4
A(16-15-19)	118.4
A(16-15-53)	103.2
A(15-16-54)	110.1
A(15-16-55)	111.4
A(19-15-53)	99.2
A(15-19-20)	116.5
A(15-19-24)	130.5
A(15-19-42)	98.6
A(54-16-55)	105.8
A(78-17-79)	107.1
A(78-17-80)	108.1
A(79-17-80)	107.2
A(58-18-59)	107.1
A(58-18-60)	107.8
A(59-18-60)	106.5
A(20-19-24)	106.9
A(20-19-42)	99.2
A(19-20-21)	105.4
A(19-20-23)	96.9
A(19-20-29)	120.8
A(24-19-42)	96.8
A(19-24-25)	100.2
A(19-24-26)	125.3
A(19-24-37)	106.3
A(21-20-23)	117.4
A(21-20-29)	110.3
A(20-21-22)	114.2
A(20-21-46)	110.9
A(20-21-47)	108.3
A(23-20-29)	105.9
A(20-23-25)	103.0
A(20-23-40)	110.6
A(20-23-41)	113.5

A(20-29-43)	113.1
A(20-29-44)	112.8
A(20-29-45)	108.8
A(22-21-46)	108.0
A(22-21-47)	108.9
A(21-22-48)	105.7
A(21-22-49)	108.6
A(46-21-47)	106.2
A(48-22-49)	105.7
A(25-23-40)	110.9
A(25-23-41)	111.6
A(23-25-24)	107.5
A(23-25-38)	111.8
A(23-25-39)	109.3
A(40-23-41)	107.3
A(25-24-26)	112.1
A(25-24-37)	107.7
A(24-25-38)	111.6
A(24-25-39)	109.7
A(26-24-37)	104.3
A(24-26-27)	113.2
A(24-26-28)	126.4
A(38-25-39)	107.0
A(27-26-28)	120.4
A(26-27-34)	110.7
A(26-27-35)	111.4
A(26-27-36)	111.7
A(26-28-32)	122.5
A(26-28-33)	121.2
A(34-27-35)	108.0
A(34-27-36)	107.0
A(35-27-36)	107.9
A(32-28-33)	116.3
A(43-29-44)	108.4
A(43-29-45)	107.4
A(44-29-45)	106.0
A(50-30-51)	107.1
A(50-30-52)	107.1
A(51-30-52)	107.6

Table A.6. Higher Occupied Molecular Orbital and Lower Unoccupied Molecular Orbital Energies, Occupancies and Symmetries.

Orbital Number	Energy (Ev)	(Occupancy)	(Symmetry)
1	-559.059056608	Occupied	A
2	-306.84072276	Occupied	A
3	-305.863282088	Occupied	A
4	-305.807770424	Occupied	A
5	-305.783007868	Occupied	A
6	-305.769674184	Occupied	A
7	-305.712257708	Occupied	A
8	-305.639874852	Occupied	A
9	-305.605860352	Occupied	A
10	-305.400957004	Occupied	A

11	-305.38626274	Occupied	A	66	-17.6535255	Occupied	A
12	-305.329390496	Occupied	A	67	-17.372157556	Occupied	A
13	-305.28149808	Occupied	A	68	-17.29025064	Occupied	A
14	-305.27061344	Occupied	A	69	-17.072285724	Occupied	A
15	-305.221360444	Occupied	A	70	-16.77050908	Occupied	A
16	-305.16720936	Occupied	A	71	-16.616219308	Occupied	A
17	-305.1440795	Occupied	A	72	-16.308183996	Occupied	A
18	-305.132922744	Occupied	A	73	-16.103280648	Occupied	A
19	-305.122854452	Occupied	A	74	-15.95824282	Occupied	A
20	-305.088023604	Occupied	A	75	-15.900009996	Occupied	A
21	-305.065710092	Occupied	A	76	-15.70381436	Occupied	A
22	-305.0624447	Occupied	A	77	-15.64667	Occupied	A
23	-305.029246548	Occupied	A	78	-15.396051164	Occupied	A
24	-304.974279116	Occupied	A	79	-15.304348072	Occupied	A
25	-304.958224272	Occupied	A	80	-15.154412156	Occupied	A
26	-304.80937682	Occupied	A	81	-15.045021524	Occupied	A
27	-304.74134782	Occupied	A	82	-14.908147176	Occupied	A
28	-304.685291924	Occupied	A	83	-14.769640132	Occupied	A
29	-304.66651592	Occupied	A	84	-14.7486872	Occupied	A
30	-304.620800432	Occupied	A	85	-14.61126862	Occupied	A
31	-304.5930446	Occupied	A	86	-14.508680888	Occupied	A
32	-36.848316024	Occupied	A	87	-14.409086432	Occupied	A
33	-31.651444656	Occupied	A	88	-14.339968968	Occupied	A
34	-31.24299854	Occupied	A	89	-14.197380184	Occupied	A
35	-30.417942828	Occupied	A	90	-14.18268592	Occupied	A
36	-29.556695688	Occupied	A	91	-13.9867624	Occupied	A
37	-29.1096091	Occupied	A	92	-13.92689688	Occupied	A
38	-28.890827836	Occupied	A	93	-13.779410008	Occupied	A
39	-28.449183568	Occupied	A	94	-13.64389624	Occupied	A
40	-27.843997584	Occupied	A	95	-13.549199872	Occupied	A
41	-27.344120492	Occupied	A	96	-13.45205446	Occupied	A
42	-27.062480432	Occupied	A	97	-13.337493624	Occupied	A
43	-26.276609424	Occupied	A	98	-13.1704144	Occupied	A
44	-26.204226568	Occupied	A	99	-13.068915132	Occupied	A
45	-25.373728536	Occupied	A	100	-12.970681256	Occupied	A
46	-25.339986152	Occupied	A	101	-12.75135576	Occupied	A
47	-25.14215782	Occupied	A	102	-12.689857544	Occupied	A
48	-25.105694276	Occupied	A	103	-12.624549704	Occupied	A
49	-24.921471744	Occupied	A	104	-12.516791768	Occupied	A
50	-24.834394624	Occupied	A	105	-12.309711492	Occupied	A
51	-24.462684168	Occupied	A	106	-12.2112055	Occupied	A
52	-23.164690848	Occupied	A	107	-12.114332204	Occupied	A
53	-22.798150596	Occupied	A	108	-12.034602216	Occupied	A
54	-22.24956474	Occupied	A	109	-11.902081724	Occupied	A
55	-21.73798666	Occupied	A	110	-11.71731496	Occupied	A
56	-21.65907302	Occupied	A	111	-11.52683376	Occupied	A
57	-20.898780916	Occupied	A	112	-11.474315372	Occupied	A
58	-20.462034736	Occupied	A	113	-11.15539542	Occupied	A
59	-19.70664072	Occupied	A	114	-11.041650932	Occupied	A
60	-19.113155724	Occupied	A	115	-10.700145352	Occupied	A
61	-18.871788832	Occupied	A	116	-10.359728236	Occupied	A
62	-18.653279684	Occupied	A	117	-10.138770044	Occupied	A
63	-18.172450712	Occupied	A	118	-10.024481324	Occupied	A
64	-17.920471296	Occupied	A	119	-9.152349544	Occupied	A
65	-17.724003544	Occupied	A	120	5.041221016	Unoccupied	A

121	5.391434308	Unoccupied	A
122	5.762872648	Unoccupied	A
123	6.165332212	Unoccupied	A
124	6.307920996	Unoccupied	A
125	6.437720328	Unoccupied	A
126	6.671740088	Unoccupied	A
127	6.730245028	Unoccupied	A
128	6.811335596	Unoccupied	A
129	7.055423648	Unoccupied	A
130	7.14440558	Unoccupied	A
131	7.235020208	Unoccupied	A
132	7.365363772	Unoccupied	A
133	7.53489204	Unoccupied	A
134	7.561559408	Unoccupied	A
135	7.593669096	Unoccupied	A
136	7.89000342	Unoccupied	A
137	8.003203676	Unoccupied	A
138	8.097083696	Unoccupied	A
139	8.263890804	Unoccupied	A
140	8.341171748	Unoccupied	A
141	8.40974498	Unoccupied	A
142	8.553150112	Unoccupied	A
143	8.626349316	Unoccupied	A
144	8.720773568	Unoccupied	A
145	8.860913308	Unoccupied	A
146	8.936833672	Unoccupied	A
147	9.018740588	Unoccupied	A
148	9.043503144	Unoccupied	A
149	9.129763916	Unoccupied	A
150	9.194527524	Unoccupied	A
151	9.250039188	Unoccupied	A
152	9.331673988	Unoccupied	A
153	9.54718986	Unoccupied	A
154	9.567054328	Unoccupied	A
155	9.760256688	Unoccupied	A
156	9.850327084	Unoccupied	A
157	9.908832024	Unoccupied	A
158	9.923254172	Unoccupied	A
159	10.00434474	Unoccupied	A
160	10.08597954	Unoccupied	A
161	10.186934576	Unoccupied	A
162	10.232650064	Unoccupied	A
163	10.331972404	Unoccupied	A
164	10.358639772	Unoccupied	A
165	10.537147868	Unoccupied	A
166	10.648171196	Unoccupied	A
167	10.7553849	Unoccupied	A
168	10.869129388	Unoccupied	A
169	10.881374608	Unoccupied	A
170	10.921103544	Unoccupied	A
171	11.171994496	Unoccupied	A
172	11.30233806	Unoccupied	A
173	11.362475696	Unoccupied	A
174	11.439212408	Unoccupied	A
175	11.572277132	Unoccupied	A
176	11.591869484	Unoccupied	A
177	11.75269004	Unoccupied	A
178	11.866162412	Unoccupied	A
179	11.94317124	Unoccupied	A
180	12.1227678	Unoccupied	A
181	12.165762128	Unoccupied	A
182	12.29420088	Unoccupied	A
183	12.306990332	Unoccupied	A
184	12.430803112	Unoccupied	A
185	12.592984248	Unoccupied	A
186	12.885781064	Unoccupied	A
187	12.997076508	Unoccupied	A
188	13.34320806	Unoccupied	A
189	13.514913256	Unoccupied	A
190	13.558723932	Unoccupied	A
191	13.593826896	Unoccupied	A
192	13.923903604	Unoccupied	A
193	14.051798124	Unoccupied	A
194	14.172617628	Unoccupied	A
195	14.469496184	Unoccupied	A
196	14.777531496	Unoccupied	A
197	14.848825888	Unoccupied	A
198	15.089104316	Unoccupied	A
199	15.390608844	Unoccupied	A
200	15.538912064	Unoccupied	A
201	15.878240716	Unoccupied	A
202	16.06436806	Unoccupied	A
203	16.297843588	Unoccupied	A
204	16.850239068	Unoccupied	A
205	17.020311568	Unoccupied	A
206	20.007601016	Unoccupied	A
207	20.154543656	Unoccupied	A
208	20.398631708	Unoccupied	A
209	20.455776068	Unoccupied	A
210	20.798642228	Unoccupied	A
211	20.884086652	Unoccupied	A
212	21.160284392	Unoccupied	A
213	21.462333152	Unoccupied	A
214	21.48900052	Unoccupied	A
215	21.726829904	Unoccupied	A
216	21.857173468	Unoccupied	A
217	21.979081436	Unoccupied	A
218	22.224257952	Unoccupied	A
219	22.395691032	Unoccupied	A
220	23.136118668	Unoccupied	A
221	23.16931682	Unoccupied	A
222	23.307551748	Unoccupied	A
223	23.376941328	Unoccupied	A
224	23.621301496	Unoccupied	A
225	23.775591268	Unoccupied	A
226	23.939677216	Unoccupied	A
227	24.145396912	Unoccupied	A
228	24.325265588	Unoccupied	A
229	24.399009024	Unoccupied	A
230	24.575612308	Unoccupied	A
231	24.84555138	Unoccupied	A
232	24.981065148	Unoccupied	A
233	25.036576812	Unoccupied	A

234	25.37073526	Unoccupied	A	289	33.559522048	Unoccupied	A
235	25.482847052	Unoccupied	A	290	33.625646236	Unoccupied	A
236	25.57618284	Unoccupied	A	291	33.701838716	Unoccupied	A
237	25.775099636	Unoccupied	A	292	33.773949456	Unoccupied	A
238	25.86326522	Unoccupied	A	293	34.001166316	Unoccupied	A
239	25.933471148	Unoccupied	A	294	34.1369522	Unoccupied	A
240	26.04014062	Unoccupied	A	295	34.234369728	Unoccupied	A
241	26.07415512	Unoccupied	A	296	34.258860168	Unoccupied	A
242	26.269262292	Unoccupied	A	297	34.3206305	Unoccupied	A
243	26.386272172	Unoccupied	A	298	34.459137544	Unoccupied	A
244	26.414572236	Unoccupied	A	299	34.616420592	Unoccupied	A
245	26.611039988	Unoccupied	A	300	34.67710246	Unoccupied	A
246	26.793629824	Unoccupied	A	301	34.797649848	Unoccupied	A
247	26.920980112	Unoccupied	A	302	34.832480696	Unoccupied	A
248	27.245886616	Unoccupied	A	303	34.95466078	Unoccupied	A
249	27.41704758	Unoccupied	A	304	35.093167824	Unoccupied	A
250	27.55990848	Unoccupied	A	305	35.162285288	Unoccupied	A
251	27.687258768	Unoccupied	A	306	35.261335512	Unoccupied	A
252	27.963184392	Unoccupied	A	307	35.434129172	Unoccupied	A
253	28.044002844	Unoccupied	A	308	35.534539976	Unoccupied	A
254	28.22387152	Unoccupied	A	309	35.566105432	Unoccupied	A
255	28.379521872	Unoccupied	A	310	35.646923884	Unoccupied	A
256	28.740619804	Unoccupied	A	311	35.923665856	Unoccupied	A
257	28.967836664	Unoccupied	A	312	35.950333224	Unoccupied	A
258	29.016001196	Unoccupied	A	313	36.027069936	Unoccupied	A
259	29.313151868	Unoccupied	A	314	36.219183832	Unoccupied	A
260	29.502000372	Unoccupied	A	315	36.262722392	Unoccupied	A
261	29.614656396	Unoccupied	A	316	36.442863184	Unoccupied	A
262	29.744183612	Unoccupied	A	317	36.50844314	Unoccupied	A
263	30.136030652	Unoccupied	A	318	36.676610828	Unoccupied	A
264	30.152629728	Unoccupied	A	319	36.911446936	Unoccupied	A
265	30.253040532	Unoccupied	A	320	37.117166632	Unoccupied	A
266	30.475087188	Unoccupied	A	321	37.231455352	Unoccupied	A
267	30.62529522	Unoccupied	A	322	37.472550128	Unoccupied	A
268	30.976869092	Unoccupied	A	323	37.559083016	Unoccupied	A
269	31.10149822	Unoccupied	A	324	37.692964088	Unoccupied	A
270	31.405179676	Unoccupied	A	325	37.84317212	Unoccupied	A
271	31.48790294	Unoccupied	A	326	37.864125052	Unoccupied	A
272	31.573891596	Unoccupied	A	327	38.113111192	Unoccupied	A
273	31.777434364	Unoccupied	A	328	38.509312088	Unoccupied	A
274	31.801924804	Unoccupied	A	329	38.533530412	Unoccupied	A
275	31.895260592	Unoccupied	A	330	38.855171524	Unoccupied	A
276	32.115946668	Unoccupied	A	331	39.011366108	Unoccupied	A
277	32.168737172	Unoccupied	A	332	39.109599984	Unoccupied	A
278	32.326292336	Unoccupied	A	333	39.53437306	Unoccupied	A
279	32.408471368	Unoccupied	A	334	39.72077252	Unoccupied	A
280	32.635143996	Unoccupied	A	335	40.007038552	Unoccupied	A
281	32.648749796	Unoccupied	A	336	40.275617044	Unoccupied	A
282	32.814740556	Unoccupied	A	337	40.772228744	Unoccupied	A
283	32.979370736	Unoccupied	A	338	41.095502552	Unoccupied	A
284	33.0688969	Unoccupied	A	339	41.369251248	Unoccupied	A
285	33.130395116	Unoccupied	A	340	41.779874292	Unoccupied	A
286	33.277881988	Unoccupied	A	341	42.149679936	Unoccupied	A
287	33.317338808	Unoccupied	A	342	42.688469616	Unoccupied	A
288	33.40632074	Unoccupied	A	343	42.74670244	Unoccupied	A

344	43.353793236	Unoccupied	A
345	44.019661088	Unoccupied	A
346	44.04333518	Unoccupied	A
347	44.776143568	Unoccupied	A
348	45.038463392	Unoccupied	A
349	45.13179918	Unoccupied	A
350	45.658887872	Unoccupied	A
351	46.07468112	Unoccupied	A
352	46.685037308	Unoccupied	A
353	47.149267204	Unoccupied	A
354	47.59172782	Unoccupied	A
355	48.03799806	Unoccupied	A
356	48.926184684	Unoccupied	A
357	49.266057568	Unoccupied	A
358	49.503886952	Unoccupied	A
359	49.802942436	Unoccupied	A
360	50.999164372	Unoccupied	A
361	51.573601248	Unoccupied	A
362	51.865581716	Unoccupied	A
363	53.3143273	Unoccupied	A
364	53.462086288	Unoccupied	A
365	53.798421664	Unoccupied	A
366	54.118702196	Unoccupied	A
367	55.349210748	Unoccupied	A
368	56.618631888	Unoccupied	A
369	57.554166696	Unoccupied	A
370	58.927536148	Unoccupied	A
371	59.886200816	Unoccupied	A
372	60.282401712	Unoccupied	A
373	61.199432632	Unoccupied	A
374	63.409014552	Unoccupied	A
375	65.357365112	Unoccupied	A
376	68.309007364	Unoccupied	A
377	70.593965416	Unoccupied	A
378	74.12848014	Unoccupied	A
379	78.472539964	Unoccupied	A